10-30-2015

A Study of Digital RF Phase Shifters Fabricated With Additive Manufacturing

Yaniel Vega
University of South Florida, yvega2@mail.usf.edu

A Study of Digital RF Phase Shifters Fabricated With Additive Manufacturing

by

Yaniel Vega

A thesis submitted in partial fulfillment
of the requirements for the degree of
Master of Science in Electrical Engineering
Department of Electrical Engineering
College of Engineering
University of South Florida

Major Professor: Thomas Weller, Ph.D.
Jing Wang, Ph.D.
Larry Dunleavy, Ph.D.

Date of Approval:
October 23, 2015

Keywords: 3D Printing, high-pass low-pass phase shifter, switched line phase shifter, direct digital manufacturing, fused deposition modeling

Dedication

Soli Deo Gloria.

Acknowledgments

I would like to express my sincere gratitude to Dr. Thomas Weller whose continuous support and mentorship has made this thesis possible. I would like to thank Dr. Larry Dunleavy and Dr. Jing Wang for volunteering their time to be part of my committee. I would like to thank John Stratton, Nick Arnal, Josh Stephenson, and Patrick Nesbitt, and Casey Perkowski- the work in this thesis would not have been finished without their help. I would like to thank Ramiro Ramirez, Denise Lugo, Mohamed Abdin, Maria Cordoba, and the rest of the WAMI team for their constant friendship and support. I would also like to thank the Air Force and Sciperio for their project sponsorship and support.

The work in this thesis was supported by the US Air Force Research Laboratory under contract #FA8650-14-C-2421. The material was assigned a clearance of CLEARED on 18 Feb 2015 (Case Number:88ABW-2015-0603).

Table of Contents

List of Tables

List of Figures

Abstract

Digital RF phase shifters fabricated using additive manufacturing processes are presented and studied. The purpose is to explain the performance differences between phase shifters fabricated using additive manufacturing and those fabricated with conventional subtractive techniques. All phase shifters are designed to operate at a center frequency of 2.45 GHz with a 100 MHz bandwidth. The 1-bit 45° switched line phase shifters have an average insertion loss of 1.3 dB and a 220 mm^2 footprint, while the 1-bit 180° high-pass low-pass phase shifters have an insertion loss 1.56 dB and a 180 mm^2 footprint. The 4-bit high-pass low-pass, switched line hybrid phase shifters on the other hand show an average state insertion loss of 5.4 dB and have a 660 mm^2 foot print. By carefully analyzing the performance of the various phase shifter designs it is shown that the limiting factors of additive manufacturing technology are the low conductivity of CB028 silver ink in comparison to copper, and the inability to print dielectrics with low surface roughness. Finally, parallel plate capacitors and a spiral inductor designed to be fabricated using additive manufacturing techniques are studied. This is done in order to better understand the advantages and disadvantages of such a design. By analyzing the component's simulated performance it is shown that 3D printed capacitors and inductors are feasible as long as the capacitance or inductance values needed are low. Large value 3D printed components are impractical for RF applications due to their large size.

Chapter 1: Introduction

In the last few years Three Dimensional (3D) printing also known as additive manufacturing has evolved from an almost unknown technology into a very popular subject of public interest. Inexpensive table-top 3D printers have made additive manufacturing technology readily available, becoming very popular with artists, hobbyists, and garage inventors everywhere. Industry has also benefited greatly from this technology. Additive manufacturing is currently being used by the automotive, space, defense and medical industries in applications ranging from the printing of low-cost prosthetic parts, to the development of inexpensive medical equipment (Figure 1.1) [1] [2]. The RF and Microwave industry has also taken a special interest in this technology. Additive manufacturing has been used to fabricate a broad range of RF and microwave devices such as antennas, transmission lines, and phase shifters [3] [4]. This thesis will focus on the latter, taking special emphasis on the performance of RF phase shifters fabricated using 3D printing technology.

Figure 1.1- Inexpensive 3D printed medical equipment

Significant research has been conducted on the topic of 3D printed microwave phase shifters. Digital RF phase shifters like the 4-bit switched-line phase shifter shown in Figure 1.2 have been fabricated using printed conductive inks on thermoplastic substrates [4]. These circuits include packaged switches and several passive lumped components. Although these 3D printed devices have been shown to perform well, their performance has not been able to match that of similar circuits constructed in more conventional technologies such as PCB.

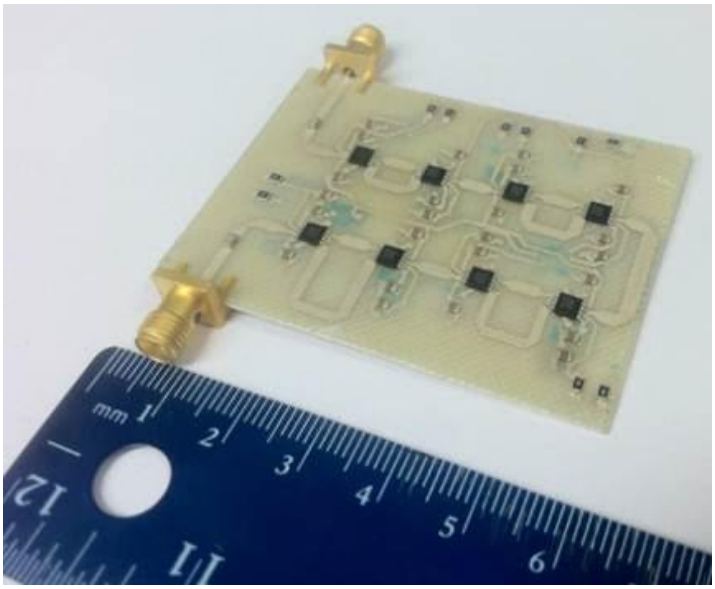

Figure 1.2- 4-bit switched-line phase shifter fabricated using silver ink on ULTEM™.

Even though 3D printed RF phase shifters like the one shown above have been fabricated and tested, a detailed examination of their performance has not previously been conducted. The detailed loss analysis presented in the main body of this thesis explains the differences in performance between circuits fabricated using additive manufacturing techniques and conventional subtractive techniques. It also provides valuable insight on the design of parallel plate capacitors and spiral inductors fabricated using additive manufacturing technology.

1.1 Thesis Contribution and Overview

The primary goal of this thesis is to study the performance of digital RF phase shifters fabricated using additive manufacturing techniques. Chapter 2 contains a brief overview of the advantages and limitations of Direct Digital Manufacturing (DDM) technology. Chapter 2 also reviews the most popular digital RF phase shifter designs with the aim of understanding their advantages and disadvantages. Chapter 3 and Chapter 4 contain the main contributions of the thesis. Chapter 3 conducts an in depth loss analysis of 3D printed digital RF phase shifters in order to better understand the performance differences between 3D printed and PCB devices. In Chapter 4 a 1-bit 180° RF phase shifter with 3D printed lumped components is designed and simulated with the intention of developing a better understanding of 3D printed lumped components and their limitations. Chapter 5 concludes the thesis and summarizes the information gathered within.

Chapter 2: Direct Print Additive Manufacturing and Phase Shifter Background

2.1 Introduction

Before venturing into the study of 3D printed digital RF phase shifters it is of great importance to at least have a rudimentary understanding of the advantages and limitations of Direct Digital Manufacturing (DDM) technology. An in-depth knowledge of digital RF phase shifters designs is also required in order to understand the behavior and performance of 3D printed phase shifters. The goal of this chapter is to provide a summary of both topics.

In Section 2.2 an overview of the fundamentals of DDM technology is given. Section 2.3 examines the most popular digital RF phase shifter designs with the aim of understanding their advantages and disadvantages. Section 2.4 takes a brief look at digital multi-bit phase shifters. Section 2.5 gives a summary of the information presented in this chapter.

2.2 Direct Digital Manufacturing (DDM)

Three Dimensional (3D) printing also known as additive manufacturing is any of the numerous fabrication processes used to make three-dimensional objects [5]. Using DDM technology multi-layer, multi-material RF structures such as filters and antennas are easily fabricated [6]. The most common 3D printing technology is Fused Deposition Modeling (FDM). In FDM, structures are manufactured one layer at a time by fusing together filaments made of thermoplastic materials such as Polylactic Acid (PLA) and Acrylonitrile Butadiene Styrene (ABS). This process is clean, simple to use, and geometries that are very difficult to manufacture

with subtractive techniques are easily achieved [7]. Table 2.1 shows the limitations of FDM technology.

Conductive inks can be used to form transmission lines for RF circuitry. This printing can be done using micro-dispensing tools such as nScrypt's SmartPump. This system uses a computer controlled valve to accurately control the deposition of material onto a substrate [8]. The limitations of this system are also shown in Table 2.1. Figures 2.1 (a) and (b) show a state of the art 3D printer, and SmartPump system made by nScrypt [8] [9].

Table 1.1- Limitations of FDM and micro-dispensing technologies

FDM Limitations		**Micro-Dispensing Limitations**	
Layer Thickness	100 µm	Line Thickness	75 µm
		Line Separation	50 µm

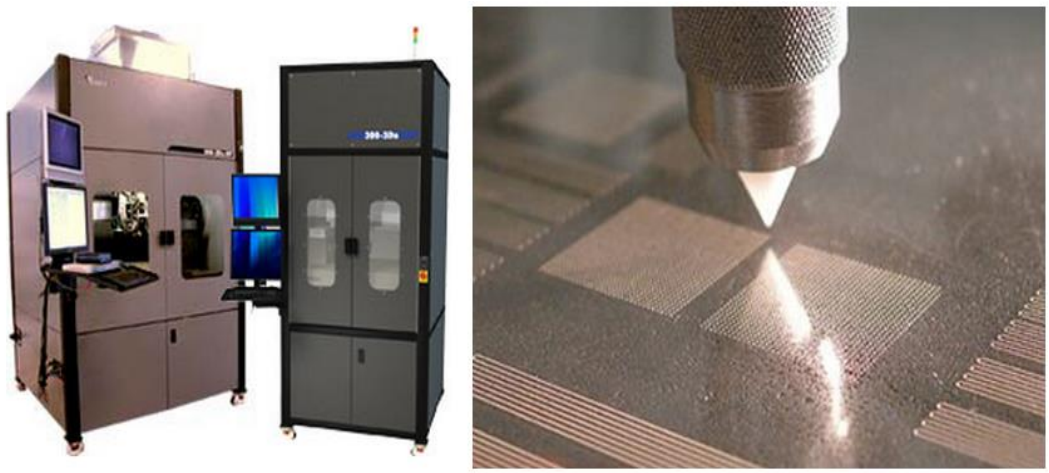

(a) (b)

Figure 2.1- NScrypt's 3Dn 3D printer (a) and SmartPump (b)

2.3 Overview of Common Phase Shifter Topologies

2.3.1 Loaded Line Phase Shifter

The loaded line phase shifter is a relatively simple phase shifter design. This type of phase shifter works on the premise that by adding a shunt capacitor or inductor to a transmission line the incident wave undergoes a phase shift [10]. By adding a negative susceptance (inductor) the incident wave undergoes a positive phase shift, while by adding a positive susceptance (capacitor) it experiences a negative phase shift. Figure 2.2 below shows a shunt loaded line phase shifter, the most common topology for this design.

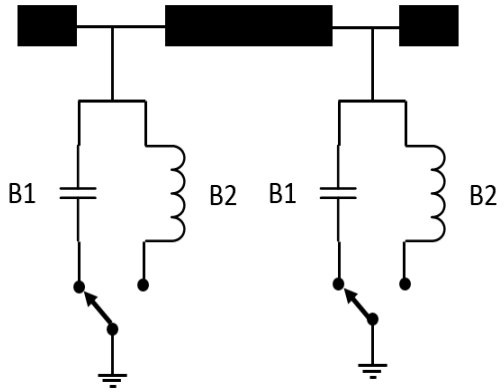

Figure 2.2- Shunt loaded line phase shifter.

The normalized susceptance B can be calculated with the following equation:

$$B = \frac{Z_{\circ}}{2\tan(\Delta\theta)} \tag{2.1}$$

where Z_o= characteristic impedance of the system, and $\Delta\theta$ is the desired phase shift.

While the capacitor and inductor values can be calculated by:

$$L = \frac{B}{2\pi f} \qquad C = \frac{1}{2\pi f B} \tag{2.2}$$

The insertion loss of the phase shifter is given by:

$$IL = 10log_{10}(1 + \frac{b^2}{4}) \quad (2.3)$$

Loaded line phase shifters are best used in applications where the required phase shift is 45° or less. They offer low insertion loss, and good power handling capability. Their large foot print on the other hand makes this design impractical for applications where space is limited.

2.3.2 Quadrature Reflection Phase Shifter

The quadrature reflection phase shifter as seen in Figure 2.3, is one of the most common reflection type phase shifter designs. It consists of a quadrature hybrid coupler that splits the incident signal into two separate signals of equal amplitude and 90° phase difference [10][11]. These two signal reflect from two switchable loads and add up in phase at the phase shifter's output if both of the loads are identical.

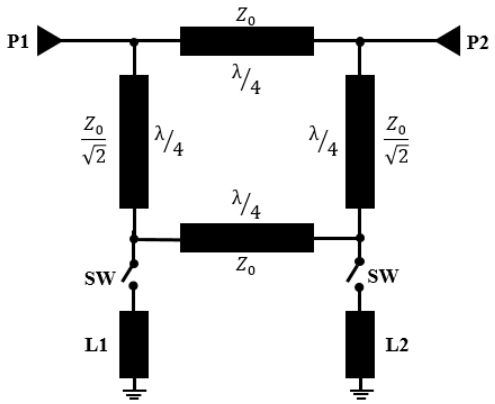

Figure 2.3- Quadrature reflection phase shifter topology

One of the best qualities of the quadrature reflection phase shifter is that it can be designed to provide any desired phase shift [11]. The coupler used in the phase shifter design can be as simple as the quadrature (90°) hybrid shown above, or as involved as a Rat-Race, or

Lange- coupler. The bandwidth of the phase shifter is dependent on the bandwidth of the coupler used [11]. The drawbacks of this phase shifter design is that at low frequencies the phase shifter can be somewhat large. The overall insertion loss of the circuit is also usually high [11].

2.3.3 Switched Line Phase Shifter

The switched line (delay line) phase shifter is the simplest phase shifter to design and implement, because it uses the time delay difference between two separate transmission lines to provide a phase shift. Figure 2.4 shows the general topology of this type of phase shifter design.

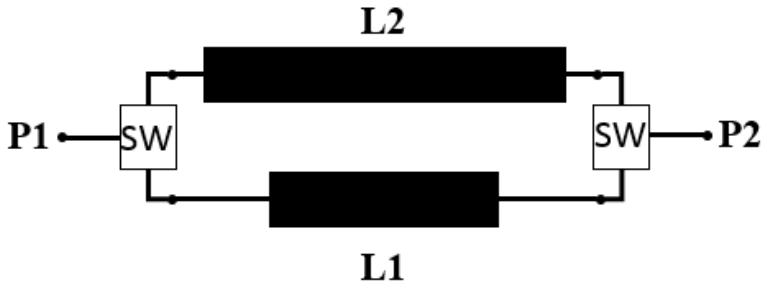

Figure 2.4- Switched line (delay line) phase shifter topology

It is common practice is to use a Single Pole Double Throw (SPDT) switch to digitally control the switching action between the reference and delay paths of the phase shifter. The switches can range from PIN diode switches to as involved as a transistor switch or a MEMS device. The switched line phase shifter can provide any desirable phase shift, but one must be careful when selecting line lengths to avoid choosing line lengths multiples of 180° which will act as a resonator when the line is in its off state [10] [11] [12].

To calculate the length difference between the reference and delay arms the following equations can be used:

$$\Delta L = \frac{\Delta\theta}{\beta} \tag{2.4}$$

where: $\beta = \frac{2\pi}{\lambda}$, $\lambda = \frac{C}{f\sqrt{\varepsilon_r}}$ (2.5-6)

The insertion loss of this phase shifter design is very low, mostly because no lumped components are used. The main disadvantage of this design is that for large phase shifts such as 90° or 180° the delay line can be quite large for low frequencies, making the design impractical for applications where space is limited.

2.3.4 High-Pass Low-Pass Phase Shifter

The high-pass low-pass phase shifter is another popular phase shifter design. As the name indicates, this phase shifter is made up of a low-pass and a high-pass filter sections. The high-pass and low-pass filters can be implemented in either the π- or T- network configurations [10] [11] [12]. Figure 2.5 shows the general topology of a low-pass high-pass phase shifter in the T-network configuration.

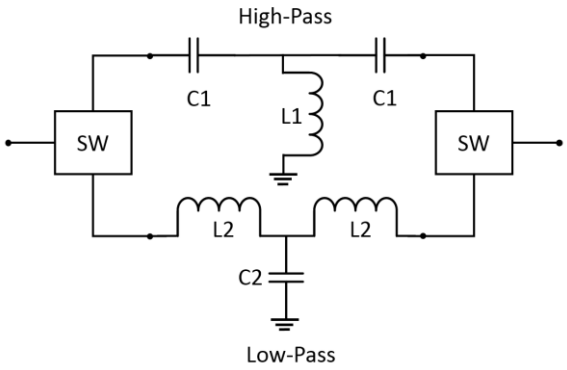

Figure 2.5- High-pass low-pass phase shifter in T-network configuration.

The capacitor and inductor values for both the high and the low pass lines are calculated by:

High-Pass Tee Low-Pass Tee

$$L_1 = \frac{Z_0}{\omega Sin(\theta)} \quad C_1 = \frac{Sin(\theta)}{\omega Z_0(1-Cos(\theta))} \qquad L_2 = Z_0\frac{(1-Cos(\theta))}{\omega Sin(\theta)} \qquad C_2 = \frac{Sin(\theta)}{\omega Z_0} \tag{2.7-10}$$

Lumped, distributed, or even 3D printed components can be used to form the high-pass and low-pass paths of the phase shifter. High-pass low-pass phase shifters offer low insertion loss, small size, and large phase shift capabilities making it one of the most popular phase shifter designs.

2.4 Digital Multi-Bit Phase Shifter

Digital multi-bit phase shifters are made by combining multiple single-bit phase shifters. Typically the phase shifters are cascaded in series with increasing phase shift angle [8]. The greater the number of cascaded bits, the larger the number of phase states that the phase shifters can produce. For example, a 2-bit phase shifter made up of 22.5° and 45° bits can produce 2^2 or 4 states at 22.5° increments (0°, 22.5°, 45°, 67.5°). On the other hand a 4-bit phase shifter as the one shown in Figure 2.6 [12] produces 2^4 or 16 states (from 0° to 360° in 22.5° increments).

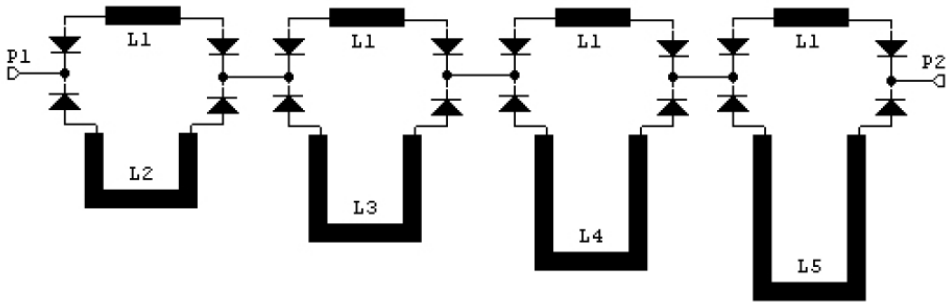

Figure 2.6- 4-bit switched-line phase shifter.

The shifting between states is typically done by turning a specific combination of switches ON and OFF. This switching action is generally performed by a digital microcontroller. The main constraint of digital multi bit phase shifters is that with a higher number of bits the complexity of the system and RF loss also increase.

2.5 Conclusion

The fundamentals of DDM technology and digital RF phase shifter design are reviewed in this chapter. In Section 2.2 the advantages and limitations of DDM technology are presented. Section 2.3 reviews several common digital RF phase shifter designs paying special attention to their performance. Section 2.4 gives a brief overview of digital multi-bit phase shifters. Table 2.2 shows a comparison of the performance and characteristics of different types of Digital RF phase shifters [12].

Table 2.1- Comparison of performance of different types of digital RF phase shifters

Type	Power Handling	Insertion Loss	Phase Shift Capability	Size
Loaded Line	High	Low	Low (~45°)	Large
Quadrature	Low	High	Large	Large
Switched Line	Medium	Low	Large	Large
High-Pass Low-Pass	Medium	Low	Medium	Small

Chapter 3: 3D Printed 4-bit Phase Shifters

3.1 Introduction

In the previous chapter the advantages and disadvantages of various digital RF phase shifter types were examined in order to choose the design that is best suited for the fabrication of a 4-bit RF digital phase shifter using DDM technology. By taking a close look at the information gathered there, it is obvious that the switched line phase shifter topology would be the best candidate for the small phase shift (22.5° and 45°) bits due to its ease of manufacturability and low loss [11]. On the other hand the high pass/low pass phase shifter topology is better suited for the larger phase shift (180° and 90°) bits due to its large phase shift capability and small size [11]. This chapter will look at the performance of digital RF phase shifter fabricated using 3D printing technology[1].

In Section 3.2 the behavior of a 1-bit 45° switched-line, a 1-bit 180° high-pass low-pass, and 4-bit digital RF DDM phase shifters will be examined. In Section 3.3 a loss analysis of the three phase shifter is performed with special emphasis on the loss contributed by the lumped components and transmission lines used in the design. Lastly, in Section 3.4 the results obtained in the previous sections will be put together in order to generate a better understanding of the performance of the 4-bit RF digital DDM phase shifter.

[1] Portions of this chapter were previously published in [6]. Permission is included in Appendix A.

3.2 Printed 4-bit RF Phase Shifter Design and Results

Before presenting the analysis of a full 4-bit, hybrid phase shifter with both high-pass low-pass and switched-line bits it would be of great interest to first observe the performance of each phase shifter topology as a standalone circuit. For this reason this section starts by demonstrating the performance of a 1-bit 45° switched-line phase shifter (Figure 3.1) and a 1-bit 180° high-pass low-pass phase shifter (Figure 3.3) before analyzing the performance of a 4-bit hybrid phase shifter made by combining four separate phase shifter bits.

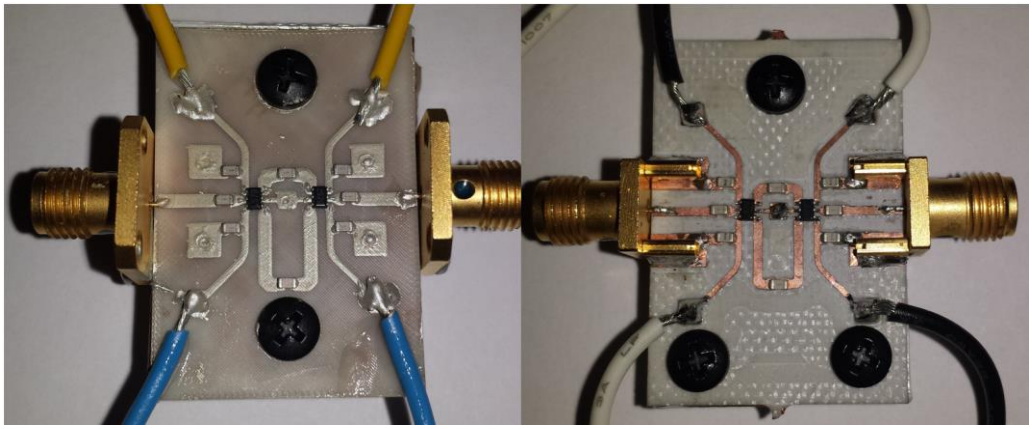

Figure 3.1-Switched-line CB028 on ABS and Cu on RO4003 phase shifters.

Two 2.45 GHz 45° switched line phase shifters were designed (Fig. 3.1). The first circuit (CB028 on ABS) was fabricated using a DDM process, while the second (Copper on RO4003) was implemented using the conventional subtractive manufacturing PCB approach, so as to compare the performance of the two technologies. The measured insertion loss, along with relative phase shift of both circuits is shown in Fig. 3.2. The DDM circuit was measured to have an insertion loss of 1.55 dB at 2.45 GHz, while the PCB circuit's insertion loss was 1.25 dB at

the same frequency. Both circuits are roughly 13 mm by 17 mm. The 0.3 dB difference between the insertion losses of the two designs will be analyzed in more detail later in the chapter.

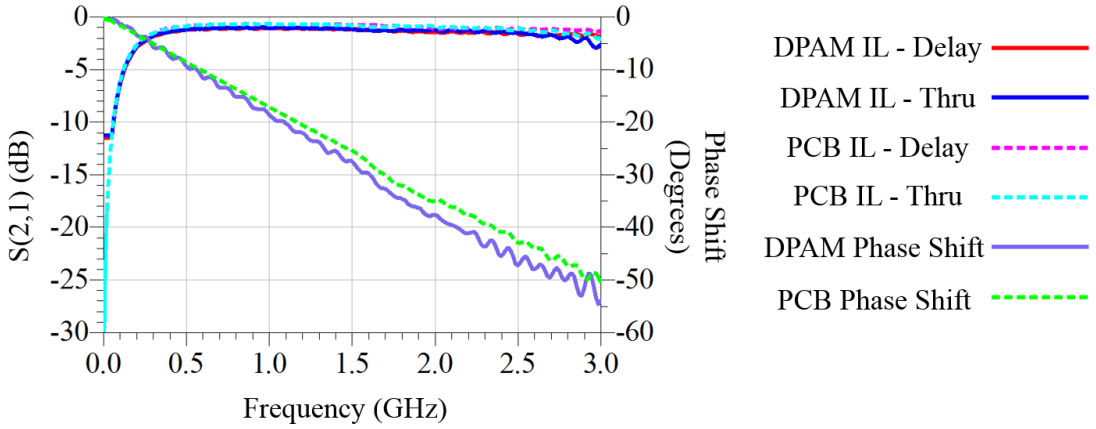

Figure 3.2- Measured IL and phase shift of DDM and PCB 45° phase shifters

Two high-pass low-pass phase shifters (Figure 3.3) were also designed and implemented using both DDM and PCB approaches. The high-pass (thru-) path is made up of two series 1.2 pF capacitors along with a 2.2 nH shunt inductor. The low-pass (delay-) path is made up of two series 3.3 nH inductors along with a 0.8 pF shunt capacitor as seen in Figure 3.6.

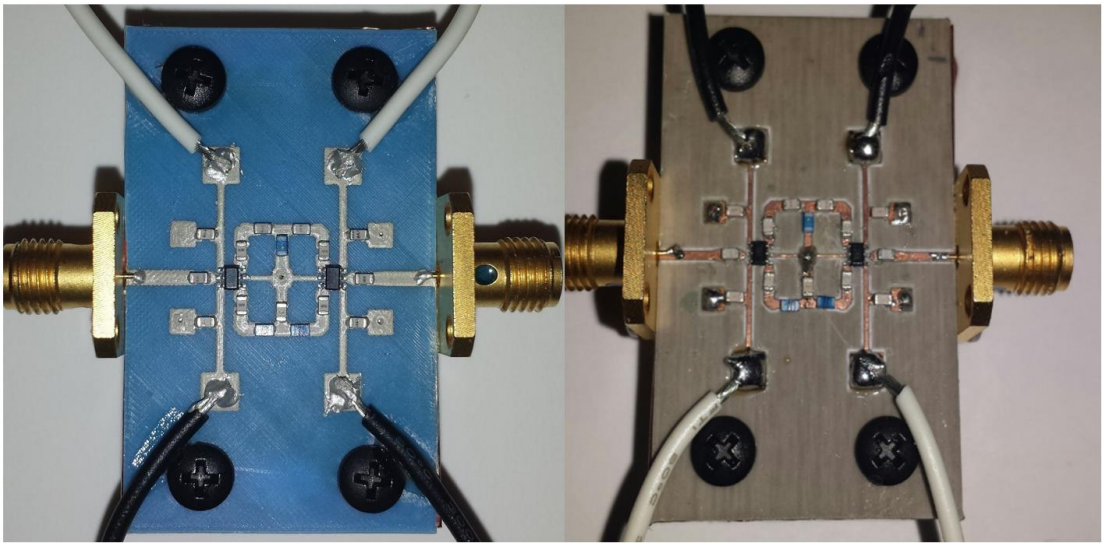

Figure 3.3- High-pass low-pass CB028 on ABS and Cu on RO4003 phase shifters

Figure 3.4 shows a measured insertion loss of around 1.56 dB and 180° relative phase shift for both circuits at 2.45 GHz center frequency. Both circuits are roughly 18 mm by 10 mm. The absence of an insertion loss difference between the two circuits will also be analyzed in detail.

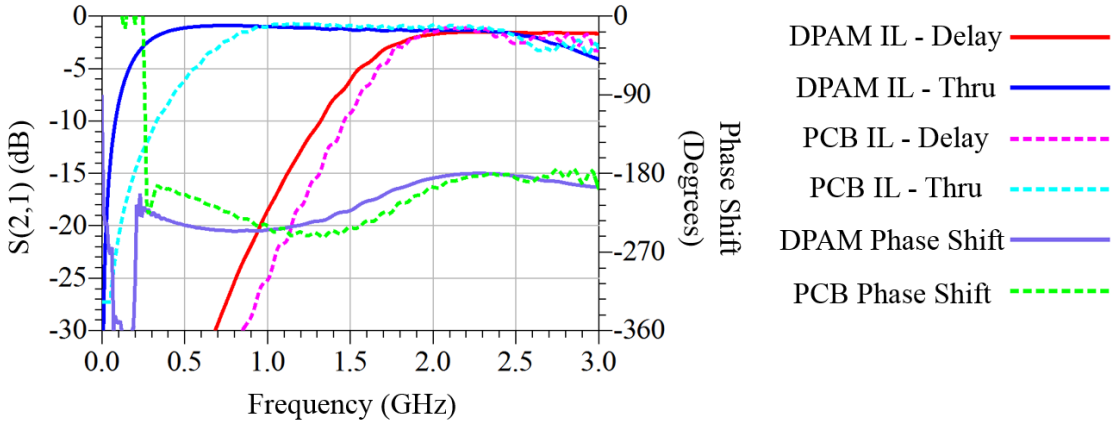

Figure 3.4- Measured IL and phase shift of DDM and PCB 180° phase shifters.

Finally 180° and 90° high-pass low-pass bits were combined with a 45° and 22.5° switched-line bits to form the 4-bit high-pass low-pass, switched-line hybrid phase shifters shown in Figure. 3.5. Once again, the phase shifter was implemented in DDM and PCB technologies in order to compare and contrast the performance of the two circuits.

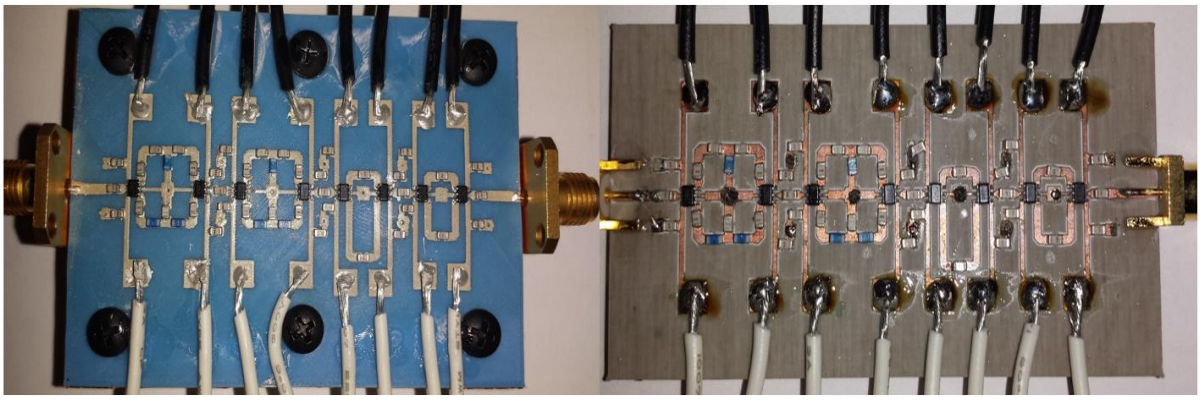

Figure 3.5- 4-bit high-pass low-pass, switched-line DDM and PCB phase shifters

Figure 3.6 shows a simplified schematic of the design while Table 3.1 shows the inductor and capacitor values used to construct the 180° and 90° high-pass low-pass bits. Table 3.2 shows the transmission line lengths and width used in the 45° and 22.5° switched-line bits.

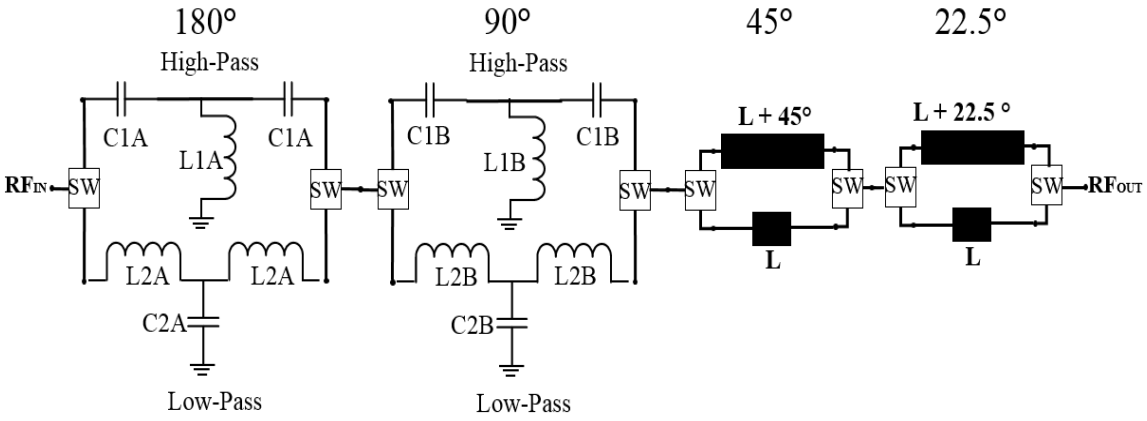

Figure 3.6- 4-bit high-pass low-pass, switched-line hybrid schematic

Table 3.1- 180° and 90° phase shifters capacitor and inductor values

180°-bit				**90°-bit**			
High Pass		**Low Pass**		**High Pass**		**Low Pass**	
C1A	1.2 pF	**C2A**	0.7 pF	**C1B**	4.7 pF	**C2B**	0.5 pF
L1A	2.2 nH	**L2A**	4.7 nH	**L1B**	2.2 nH	**L2B**	2.2 nH

The measured insertion loss for all 16 states of both circuits is shown in Figure 3.7. Figure 3.8 shows the return loss of the DDM circuit. The relative phase shift of both circuits is shown in Figure 3.9. The DDM circuit was measured to have an average insertion loss of 5.8 dB at 2.45 GHz, while the PCB circuit's average insertion loss was 5.03 dB at the same frequency. Both circuits are roughly 51 mm by 13 mm.

Table 3.2- 45° and 22.5° phase shifters transmission line lengths and widths.

45°-bit				**22.5°-bit**			
Thru Length	4.5 mm	**Delay Length**	15.2 mm	**Thru Length**	4.5 mm	**Delay Length**	9.6 mm
Thru Width	1.1 mm	**Delay Width**	1.1 mm	**Thru Width**	1.1 mm	**Delay Width**	1.1 mm

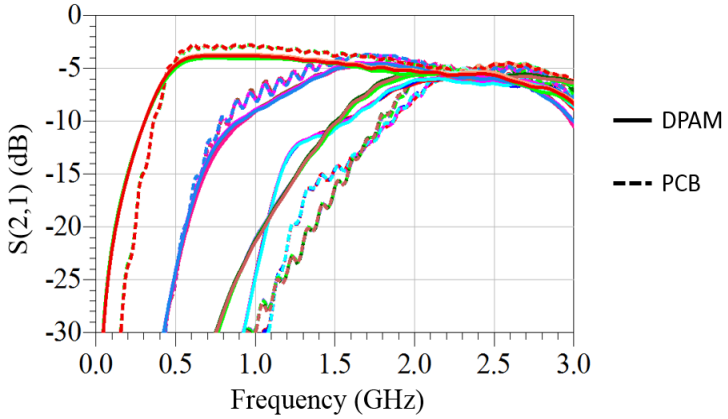

Figure 3.7- Measured insertion loss of DDM and PCB 4-bit phase shifters

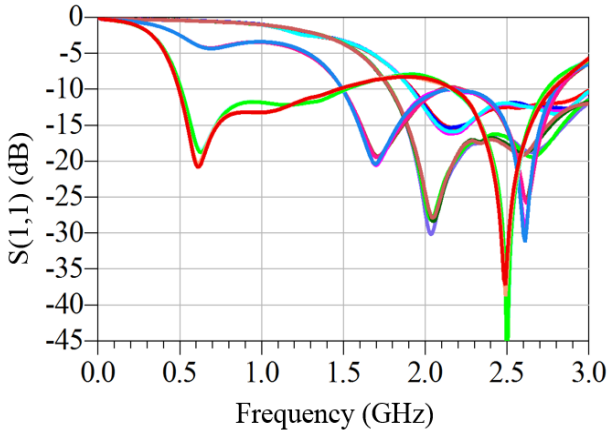

Figure 3.8- Measured return loss for all 16 stages of the DDM phase shifter

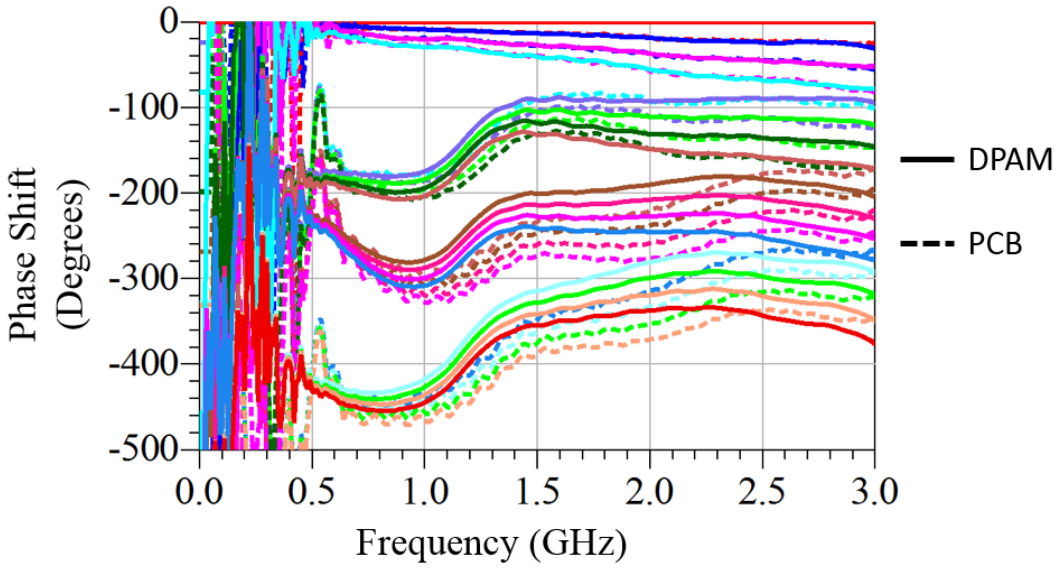

Figure 3.9- Measured relative phase shift of DDM and PCB 4-bit phase shifters

Figures 3.10 and 3.11 show the RMS phase error and RMS amplitude error vs. frequency of the 4-bit high-pass low-pass, switched-line hybrid DDM phase shifter over a 100 MHz bandwidth [13].

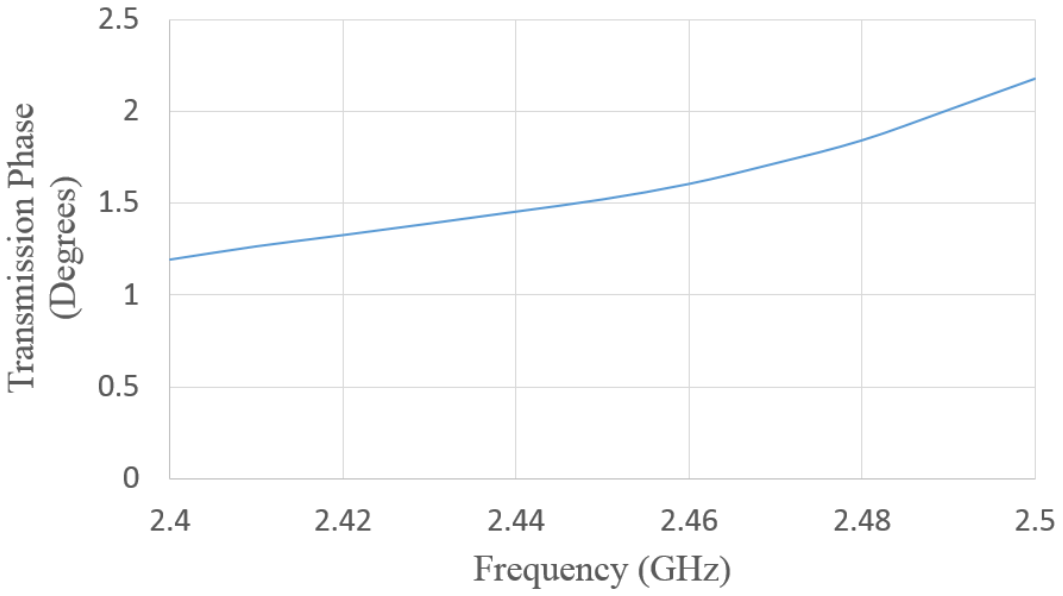

Figure 3.10 - RMS phase error vs. frequency of DDM 4-bit phase shifter.

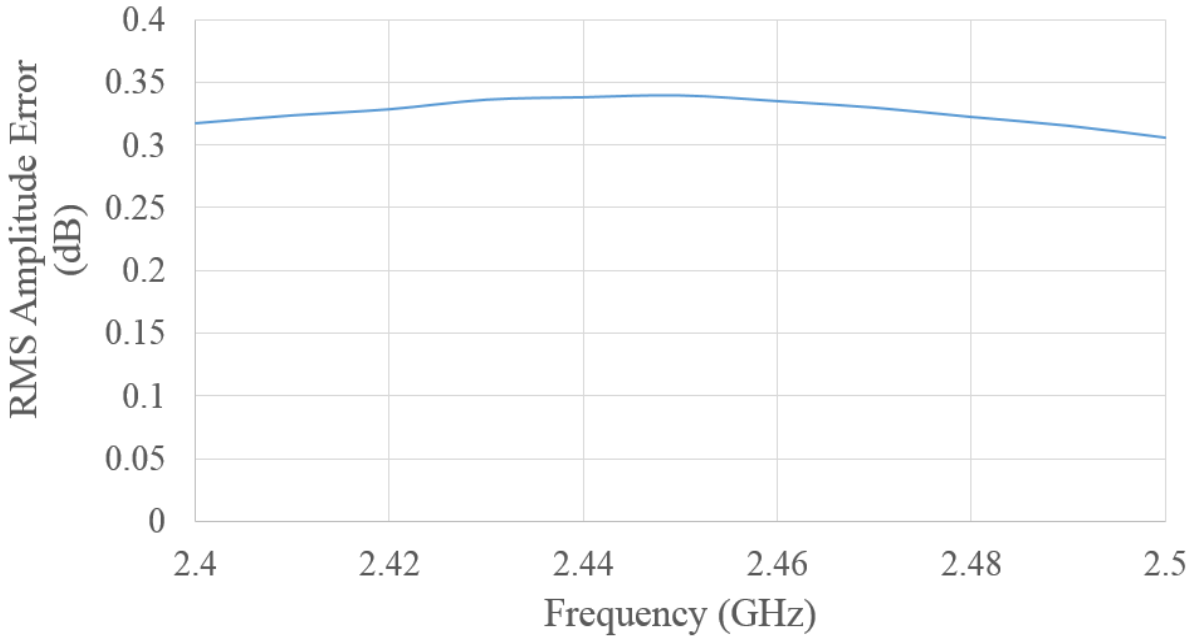

Figure 3.11- RMS magnitude error vs. frequency of DDM 4-bit phase shifter.

3.3 Loss Analysis

3.3.1 Switch Loss

The MASWSS0115 GaAs SPDT RF switch was chosen to perform the switching action between the phase shifters thru- and delay- paths. This switch was chosen because it offers a relatively low insertion loss of 0.4 dB throughout its entire operational bandwidth (DC-3 GHz), making the total insertion loss due to switches to be 3.2 dB for the 4-bit phase shifter. The switch has a maximum input power of 34 dBm (2.5 W) making it suitable to be used in low power phase array applications. The switch is also relatively small having only a 4.2 mm^2. For proper operation of the switch external DC blocking capacitors are required on all RF ports. ATC 600S 30 pF ceramic capacitors were used as DC blocks on all phase shifter designs.

3.3.2 Surface Mount Components Loss

Throughout the design a multitude of surface mount capacitors and inductors are used, to act as DC blocks in the switches' biasing networks, and to form the high-pass and low-pass branches on the 180° and 90° bits. ATC's 600S capacitors and Coilcraft 603CS inductors were chosen for all designs because of their low loss and small size. Modelithics' models for the above components were used in all phase shifter simulations. Table 3.3 shows all of the components values and quantities used in the 4-bit phase shifter.

Table 3.3- Capacitors and inductors values, and quantities.

ATC 600S Capacitors Value	**Quantity**
0.5 pF	1
0.7 pF	1
1.2 pF	2
4.7 pF	2
30 pF	17
Coilcraft 603CS Inductors Value	
2.2 nH	4
4.7 nH	2

To better understand how the surface mount components contribute to the overall insertion loss of the 4-bit phase shifter we can study in detail the 1-bit 180° high-pass low-pass phase shifters shown in Figure 3.3. By conducting a simulation of the high-pass and low-pass paths taking only the lumped components into account, an average per-path component loss of 0.32 dB is calculated. By adding this per-path components loss to the loss contributed by the switches and DC blocks a calculated insertion loss of 1.2 dB is obtained for both the DDM and PCB circuits. Note that this insertion loss is only 0.36 dB less than the measure insertion loss of

both 180° phase shifters. This 0.36 dB discrepancy can be attributed to a combination of transmission line and interconnect loss. Another point worth noting is that because the insertion loss of the DDM and PCB circuits is very similar (~1.56 dB), it can be assumed that the majority of the loss in a high-pass low-pass phase shifter design comes from the lumped components themselves and not from the transmission lines as is expected in a switched-line design.

3.3.3 Transmission Line Loss

To gain a better understanding of the transmission line loss contributed to the phase shifter a close examination of the 1-bit 45° switched-line phase shifters (Figure.3.1) is presented in this section. The single bit 45° switched-line phase shifters were chosen for this type of analysis because unlike the 180° high-pass low-pass designs the majority of the insertion loss of the circuit (excluding switch loss) can be attributed to transmission line losses, due to the nature of the switched-line design.

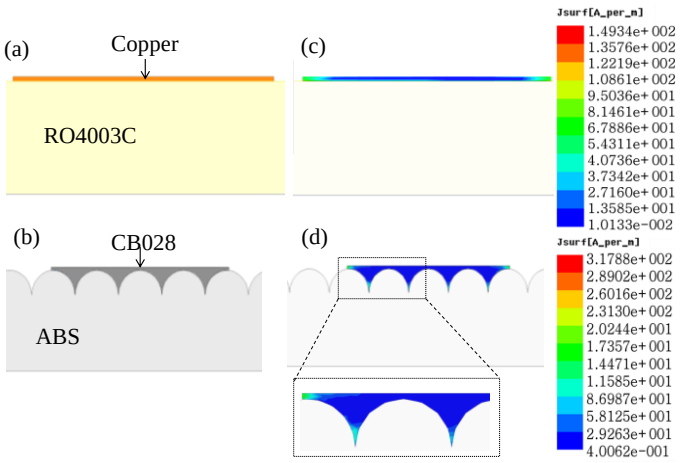

Figure 3.12- Cu on RO4003 (a), CB028 on ABS (b). Simulated surface current density for Cu on RO4003(c) and CB028 on ABS (d).

In [14] the results of full-wave EM simulations for CB028 on ABS and copper on RO4003 transmission lines is described[2]. The cross section of the two microstrip lines used in the simulations are shown in Figure 3.12 (a) and (b).

The microstrip line lengths and widths used in the simulation are those of the 45° phase shifters with DC blocking capacitors and switches removed. The microstrip line dimensions are 24.8 mm by 0.82 mm for copper on RO4003, and 27.12 mm by 1.12 mm for the CB028 on ABS. One key aspect to notice from Figure 3.12 (a) and (b) is that although both the conductive materials (CB028 and copper) are assumed to be flat on the top surface, on the DDM line the CB028 conforms to the irregular surface of the printed ABS. Previously conducted measurements show that the effective conductivity of the CB028 on ABS microstrip line is directly linked to the surface roughness of the ABS substrate [14]. The surface roughness of each of the three DDM phase shifter circuits is shown in Table 3.4.

Table 3.4- Surface roughness of each of the three DDM phase shifter circuits

Circuit	**Dielectric Surface Roughness**	**Conductor Surface Roughness**
1-bit 45° Switched-Line Phase Shifter (Fig 3.1)	2.32 μm	1.74 μm
1-bit 180° High-Pass Low-Pass Phase Shifter (Fig 3.3)	3.21 μm	3.73 μm
4-bit Hybrid Phase Shifter (Fig 3.5)	4.77 μm	4.27 μm

For the purpose of this simulations the conductivity of CB028 was designated to be 1e6 S/m, which is at the lower end of previously conducted measurements [15]. Figure 3.12 (c) and (d) show the current density of the simulated micro strip lines at 3 GHz. Note that the current

[2] Simulations performed by Maria Cordoba, USF PhD student

density is greater at the edges of the copper and CBO28 as expected, but in the case of the CB028 on ABS line, there is also a high current concentration in the crevasses formed in the ABS surface. Figure 3.13 shows the simulated insertion loss of the copper on RO4003 and CB028 on ABS microstrip lines.

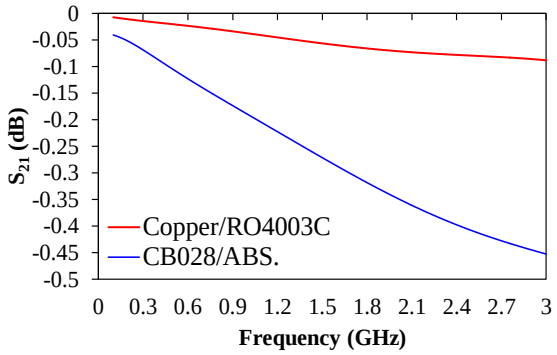

Figure 3.13- Simulated IL of Cu on RO4003 and CB028 on ABS microstrip lines.

One can observe that at the frequency of interest 2.45 GHz, the losses are around 0.32 dB higher for the CB028 on ABS that for copper on RO4003 line. This 0.32 dB difference is in accordance to the measured difference in insertion loss between both of the 1-bit 45° switched line phase shifters shown in Figure 3.2.

3.4 Conclusion

A detailed inspection of the performance of the phase shifter shown in Section 3.2 provides valuable information regarding the behavior of 3D printed digital RF phase shifters. In Section 3.3.1 it was shown that the majority of the insertion loss of a phase shifter comes from the switches. In Section 3.3.2 it was demonstrated that, not counting the switches the majority of the loss in a high-pass low-pass phase shifter comes from the lumped components that make up the high-pass and low-pass paths, explaining the similar performance of the 1-bit 180° DDM and PCB phase shifters (Figure 3.3). In Section 3.3.3 the detail study of a CB028 on ABS and copper

on RO4003 transmission lines explains the 0.3 dB difference in the insertion loss between the DDM and PCB 1-bit 45° switched-line phase shifters shown in Figure 3.1. Table 3.5 shows detailed loss analysis of all three phase shifters designs. The slight differences between the calculated and measured losses are due to interconnection losses not accounted by the simulations.

Table.3.5- Detailed loss analysis of all three phase shifter designs.

Circuit	**Total Switch Loss (dB)**	**Total Component Loss (dB)**	**Total Transmission Line Loss (dB)**	**Total Calculated Loss (dB)**	**Measured Loss (dB)**
45° Switched-Line DDM	0.8	0.045	0.43	1.27	1.55
45° Switched-Line PCB	0.8	0.045	0.1	0.95	1.25
180° High-Pass Low-Pass DDM	0.8	0.35	0.1	1.25	1.56
180° High-Pass Low-Pass PCB	0.8	0.35	0.1	1.25	1.56
4-bit Hybrid DDM	3.2	0.7	1.55	5.45	5.80
4-bit Hybrid PCB	3.2	0.7	0.4	4.3	5.03

In conclusion, DDM technology has been shown to be comparable to the more conventional subtractive manufacturing processes such as PCB for the presented digital RF phase shifters. The main constraining factors to the technology are shown to be the lower conductivity of CB028 in comparison to copper, and the inability to print dielectrics with low surface roughness.

Chapter 4: 1-Bit 180° RF Phase Shifter with 3D Printed Lumped Components

4.1 Introduction

By comparing the performance of multiple 3D printed and PCB circuits, the previous chapter shows that DDM technology is suitable for manufacturing digital RF phase shifters. In this chapter a 1-bit 180° RF phase shifter with 3D printed lumped components is designed and simulated with the intention of developing a better understanding of 3D printed lumped components.

In Sections 4.2 and 4.3 the design and simulations of a parallel plate capacitor and a spiral inductor are presented. The design and simulations of a 1-bit 180° RF phase shifter is shown in Section 4.4. Lastly, in Section 4.5 the data presented in this chapter is analyzed in order to understand the advantages and disadvantages of 3D printed lumped components.

4.2 3D Printed Parallel Plate Capacitor

In its simplest form a parallel plate capacitor is made up of two parallel plates separated by a dielectric. The capacitance value of a parallel plate capacitor is calculated by the following equation [16]:

$$\boldsymbol{C = \varepsilon_r \varepsilon_o \frac{A}{d}} \ \ \textbf{(F)} \tag{4.1}$$

where ε_r is the dielectric constant of the dielectric material, ε_o is the permittivity of free space or vacuum permittivity, A is the area overlapped by the parallel plates, and d is the separation between the two plates. In this section a 3D printed 1.3 pF parallel plate capacitor is designed

and simulated using Keysight's Momentum 3D planar EM simulator. The 3D printed capacitor dimensions were tuned to match the performance of a 1.3 pF ATC capacitor model. Figure 4.1 shows the layout (a) and 3D view (b) of the 3D printed parallel plate capacitor. The parallel plates are constructed using CB028 silver ink printed on both sides of a 100 µm ABS dielectric. The capacitor itself is printed on a 16 mil thick ABS substrate.

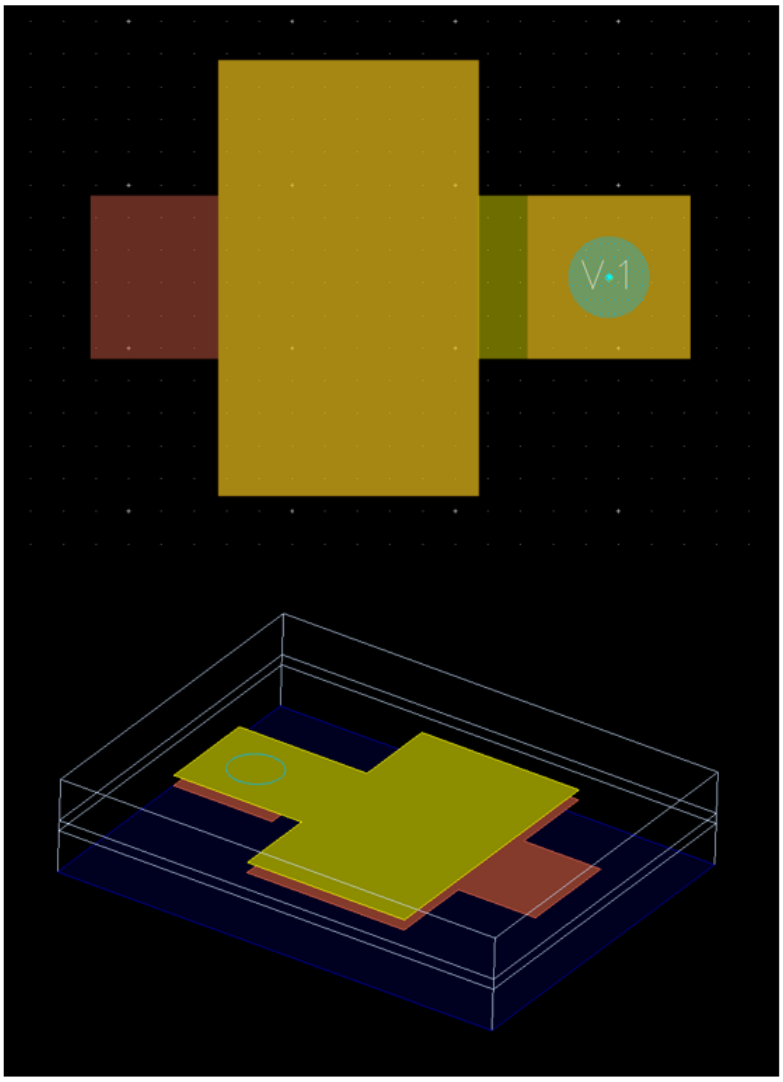

Figure 4.1- 3D printed parallel plate capacitor layout (a), 3D view (b).

In Figure 4.2 the capacitance of the simulated 3D printed parallel plate capacitor is compared to the ATC capacitor model of the same nominal value. The insertion loss and S11 are shown in Figures 4.3 and 4.4. The phase is shown in Figure 4.5.

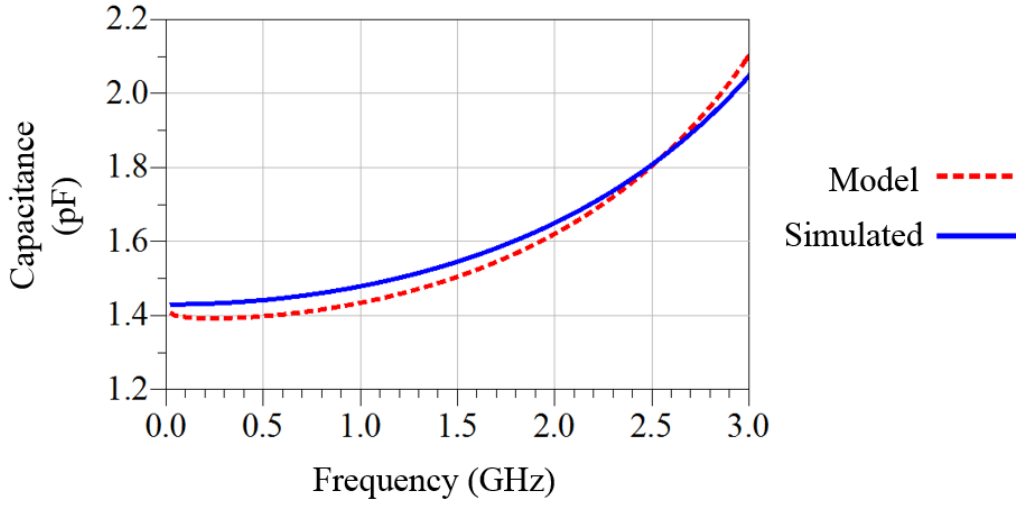

Figure 4.2- Capacitance of 1.3 pF 3D printed capacitor and ATC capacitor model.

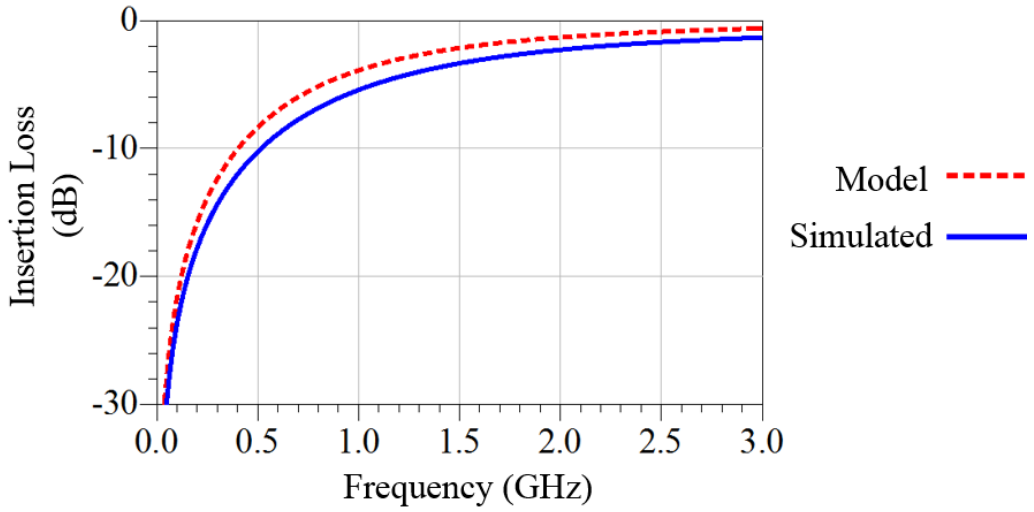

Figure 4.3- Insertion loss of 1.3 pF 3D printed capacitor and ATC capacitor model.

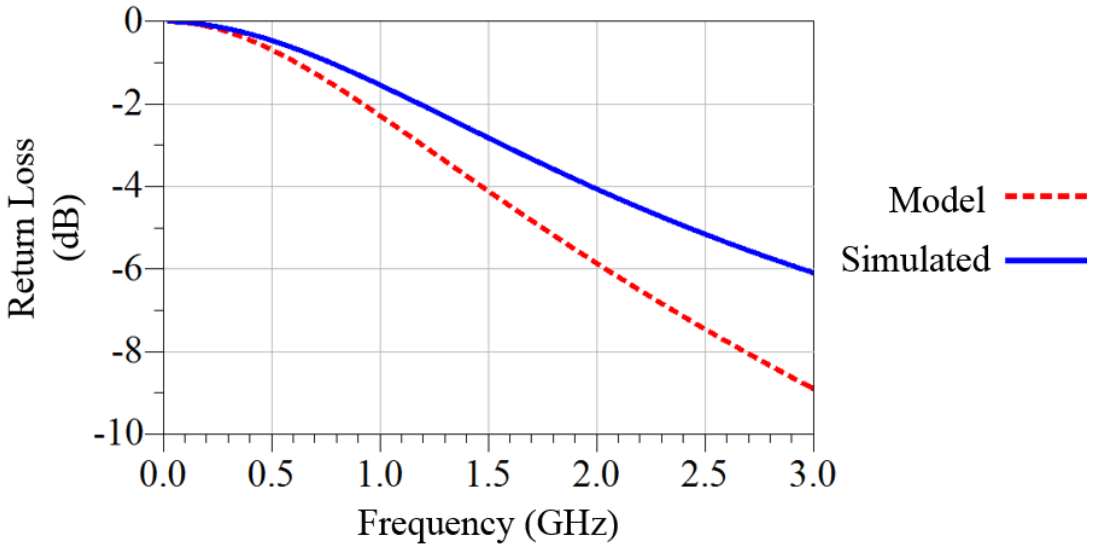

Figure 4.4- Return loss of 1.3 pF 3D printed capacitor and ATC capacitor model.

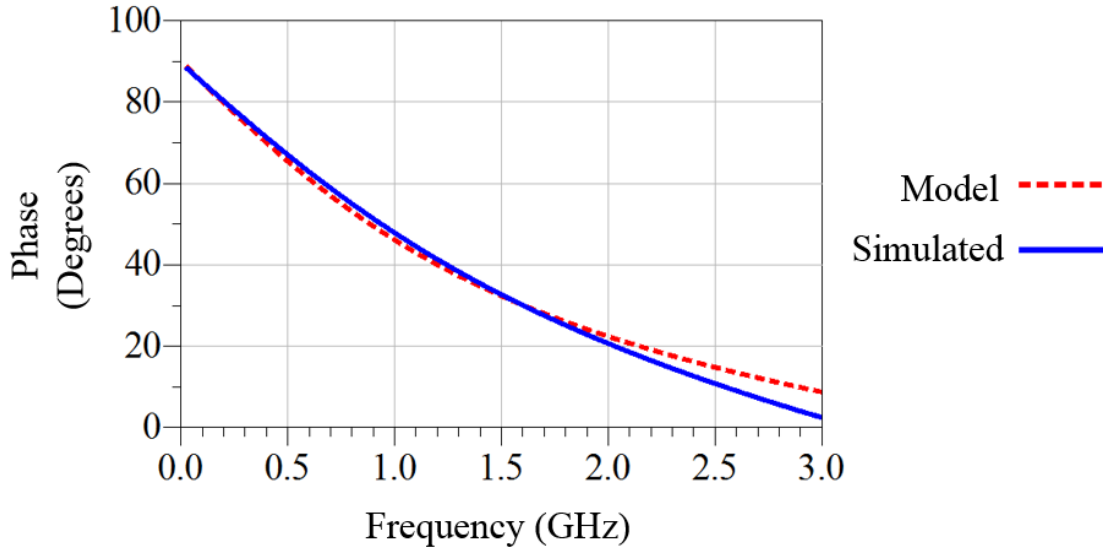

Figure 4.5- Phase of 1.3 pF 3D printed capacitor and ATC capacitor model.

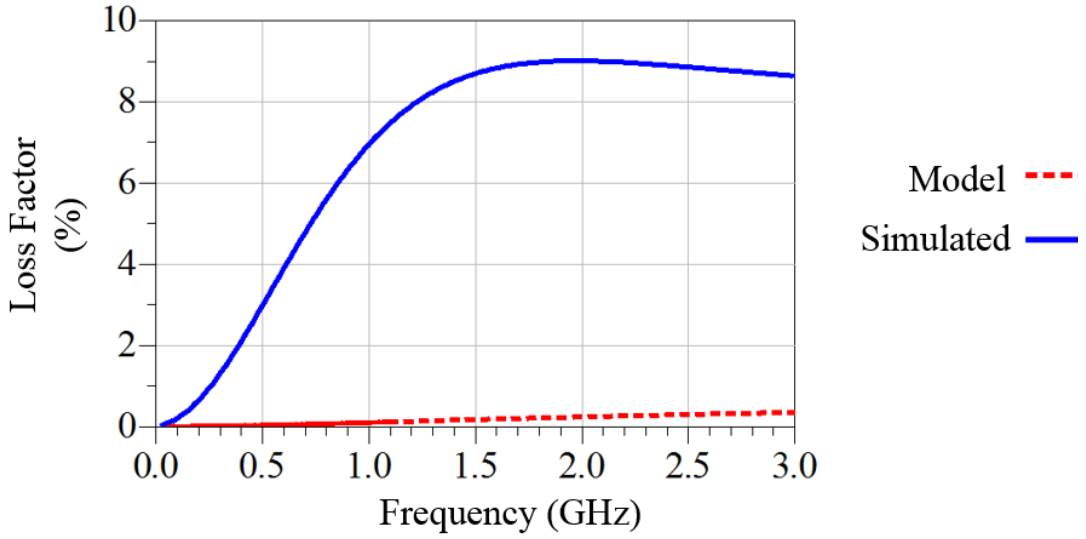

Figure 4.6- Loss Factor of 1.3 pF 3D printed capacitor and ATC capacitor model.

The 3D printed parallel plate capacitor has a simulated insertion loss of 1.7 dB at 2.45 GHz. Note that losses of the 3D printed capacitor are greater than that of the model. This can be partly attributed to the low conductivity (1E6 S/M) of CB028, high loss tangent (0.0078) of ABS, the inferior return loss (5 dB at 2.5 GHz) of the printed component and the larger dissipation loss in comparison to the ATC capacitor model. Increasing the component's capacitance would reduce the series impedance, thus making the insertion loss lower and the return loss higher. Increasing the capacitance is not an option in this case, because by doing so the capacitance of the 3D printed component would no longer match that of the ATC model. Figure 4.6 shows the capacitor's loss factor in percentage. This is the energy that is lost due to radiation loss and heat dissipation. The capacitor dimensions are 1.6 mm by 2.67 mm, having an overlapping parallel plate area (A) of 4.27 mm^2.

4.3 3D Printed Spiral Inductor

In this section a 3.25 nH 3D printed spiral inductor is designed and simulated. Conveniently enough a spiral inductor can be simply drawn in ADS by using the MRIN preset component. Once again CB028 silver ink is assumed for all conductor traces. The 3D printed spiral inductor dimensions were tuned to match the performance of a 3.25 nH Coilcraft inductor model while staying within the physical limitations of DDM technology shown in Table 2.1. Figure 4.7 shows the 3.25 nH spiral inductor Momentum layout (b) and dimensions (a). In Figure 4.8 the inductance of the simulated 3D printed spiral inductor is compared to that of a Coilcraft inductor of the same nominal value. Figure 4.9 and 4.10 show the insertion, and return loss of the 3D printed spiral inductor while Figure 4.11 shows the phase delay.

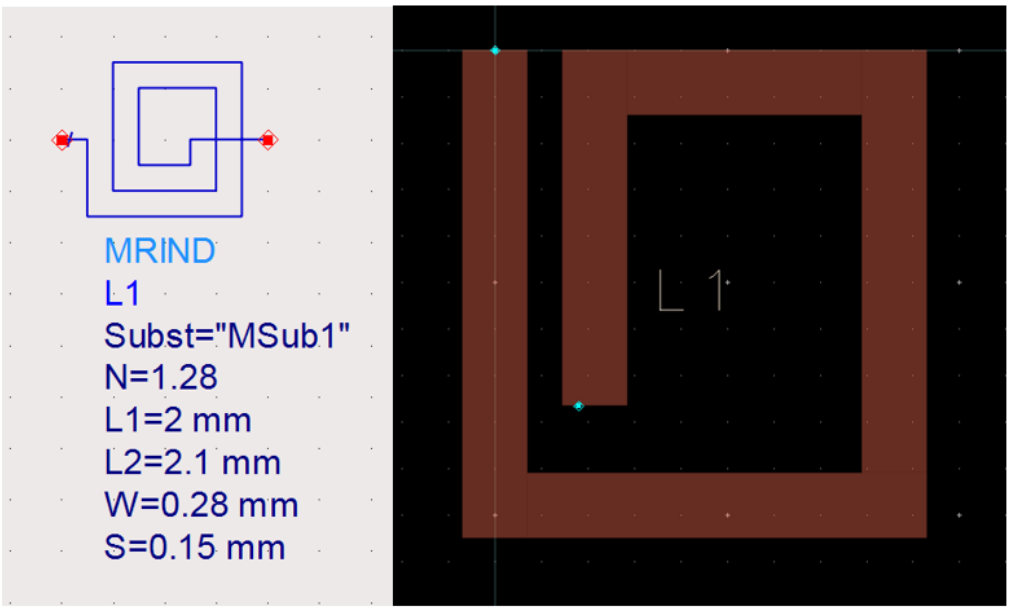

Figure 4.7- MRIND component dimensions. Where N= Number of turns, L1= Length of second outermost segment, L2= Length of outermost segment, W= Conductor width, and S= Conductor spacing. (a), 3D printed spiral inductor Momentum layout (b)

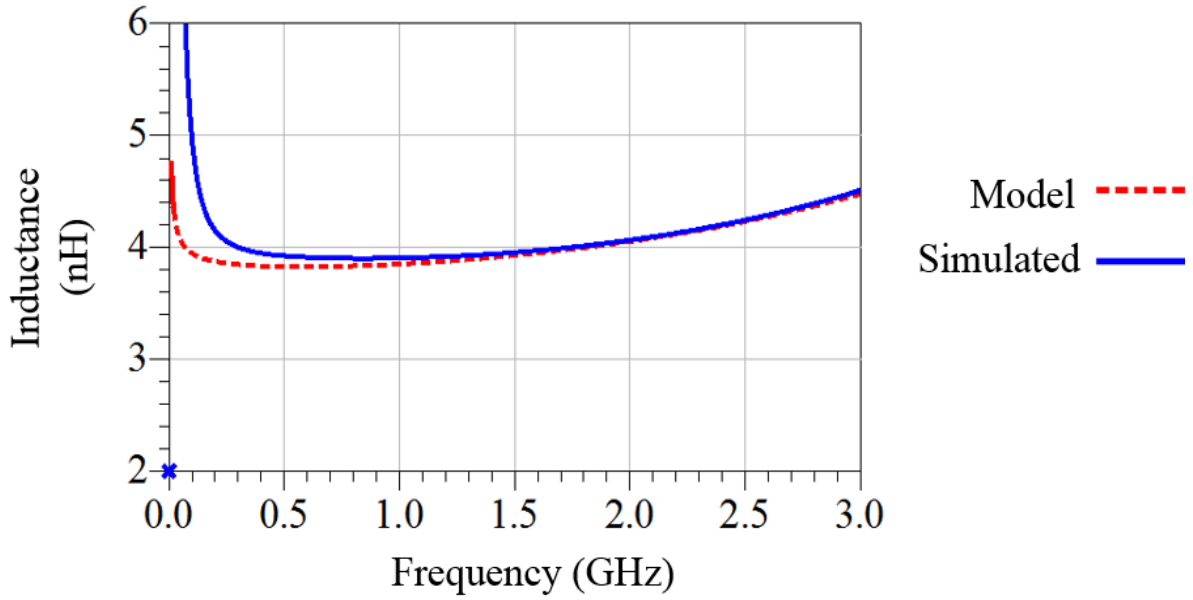

Figure 4.8- Inductance of 3.25 nH 3D printed inductor and Coilcraft inductor model.

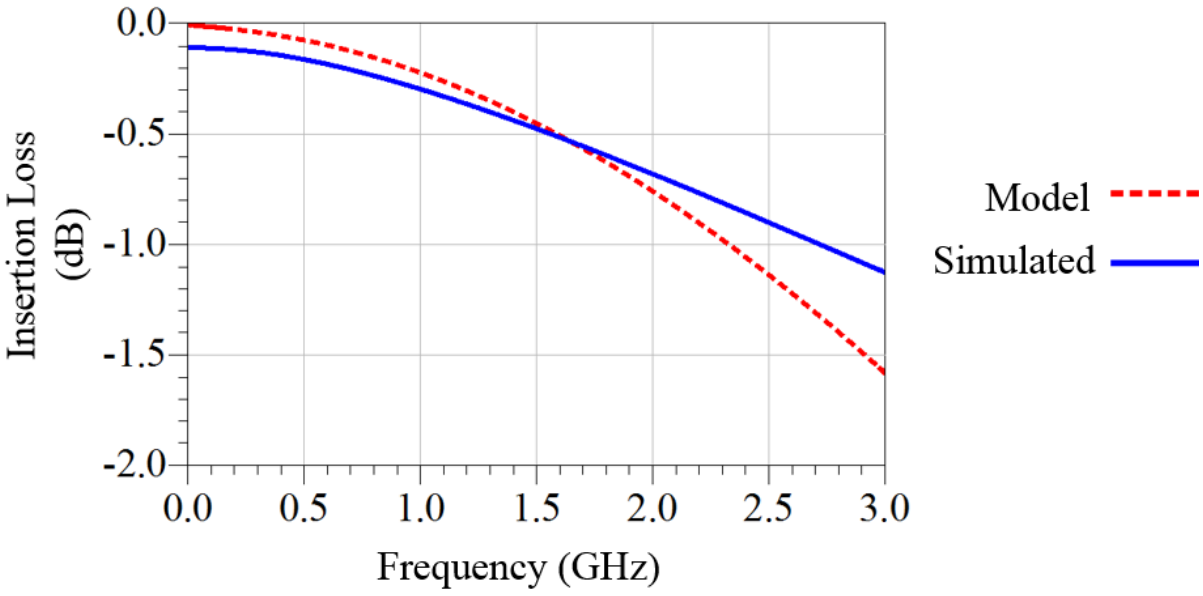

Figure 4.9- Insertion loss of 3.25 nH 3D printed inductor and Coilcraft inductor model.

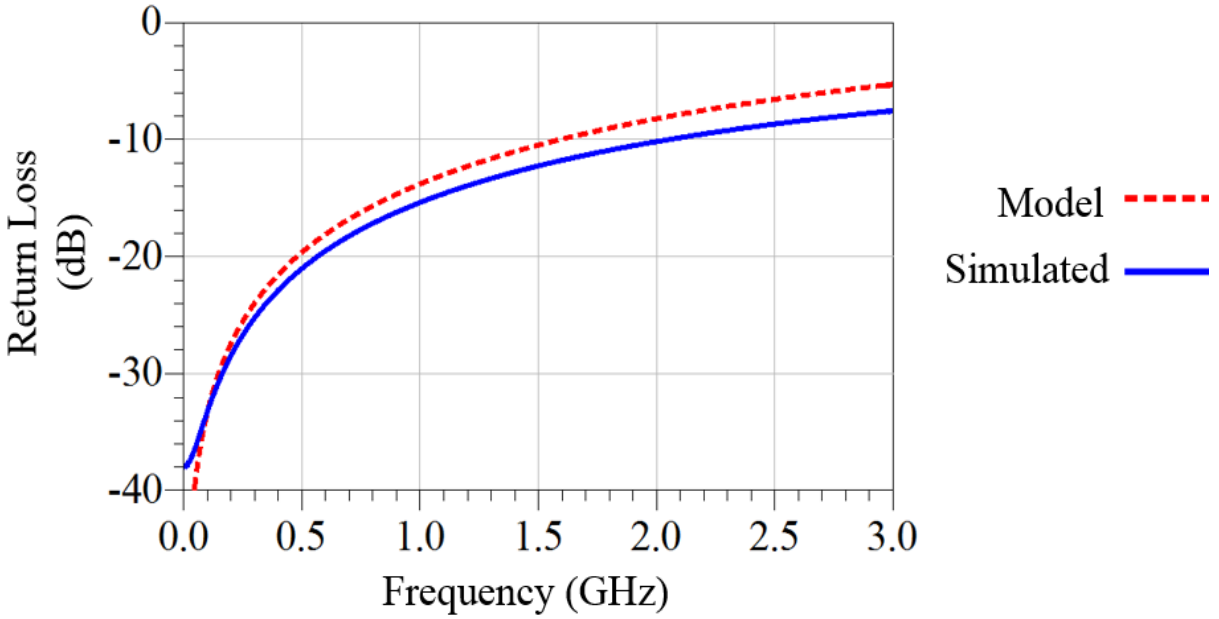

Figure 4.10- Return loss of 3.25 nH 3D printed inductor and Coilcraft inductor model.

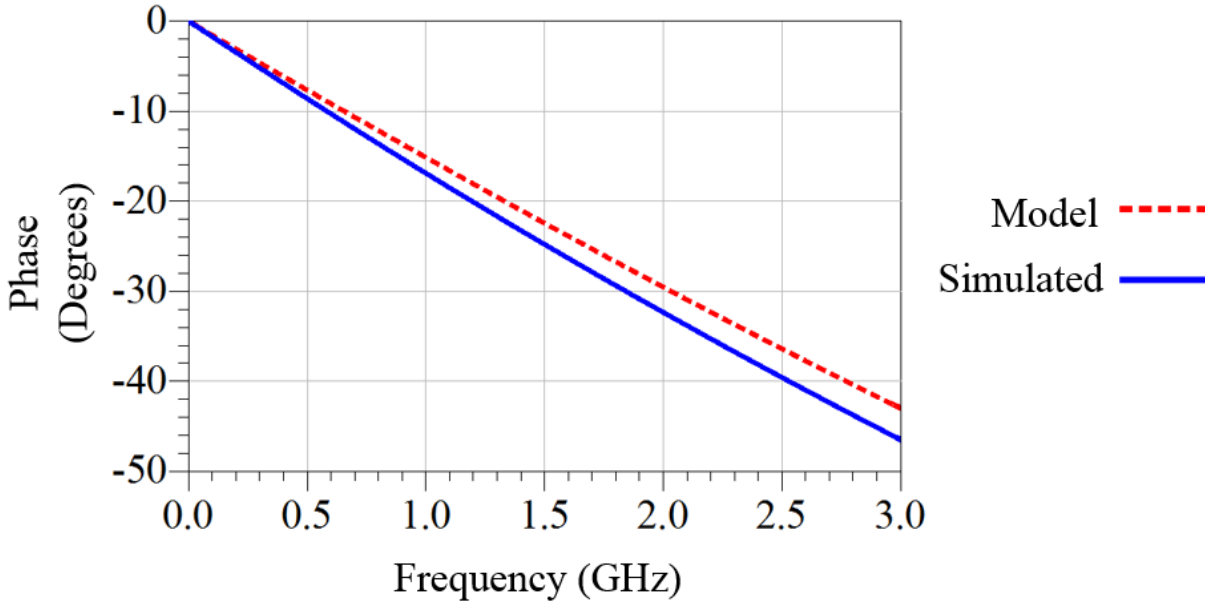

Figure 4.11- Phase of 3.25 nH 3D printed inductor and Coilcraft inductor model.

The 3D printed spiral inductor simulated insertion loss is 0.9 dB at 2.45 GHz. The simulated return loss is 8.8 dB at the same frequency. Figure 4.12 shows the loss factor in percentage.

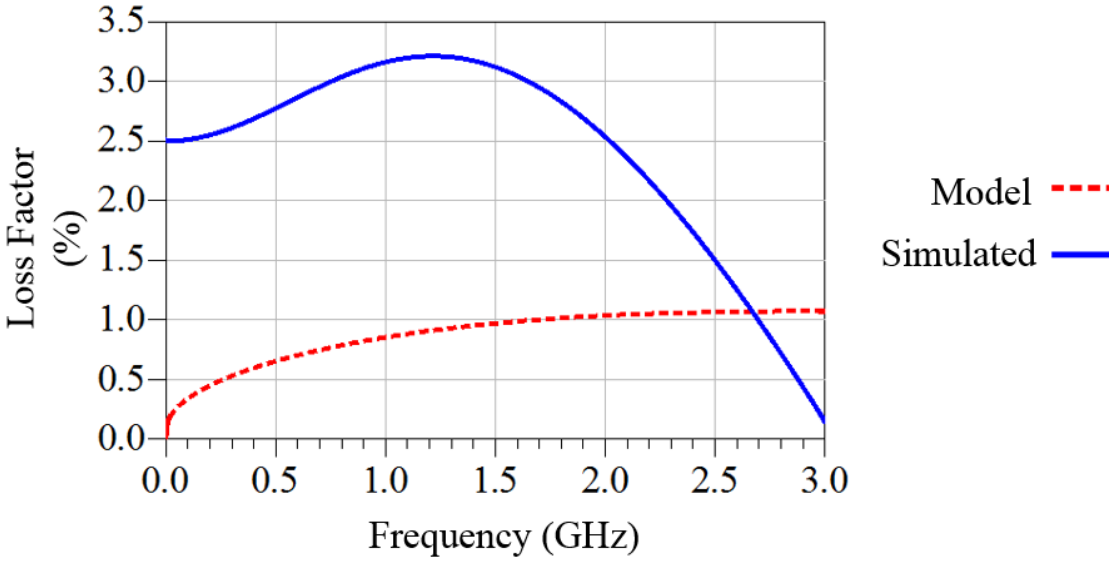

Figure 4.12- Loss Factor of 3.25 nH 3D printed inductor and Coilcraft inductor model.

4.4 1-Bit 180° Phase Shifter with 3D Printed Lumped Components

In this section a 1-bit 180° phase shifter with 3D printed lumped components is designed and simulated. The thru-path is made up of 3D printed parallel plate capacitors and spiral inductors joined together to form a high-pass filter which offers a phase advance [11]. The delay-path is made by meandering a 26.7 mm long transmission line which offers a phase delay [2]. Figure 4.13 shows the Momentum layout of the 180° phase shifter with 3D printed lumped components. Figure 4.14 show a 3D view of the same circuit. The phase shifter is roughly 20 mm by 10 mm.

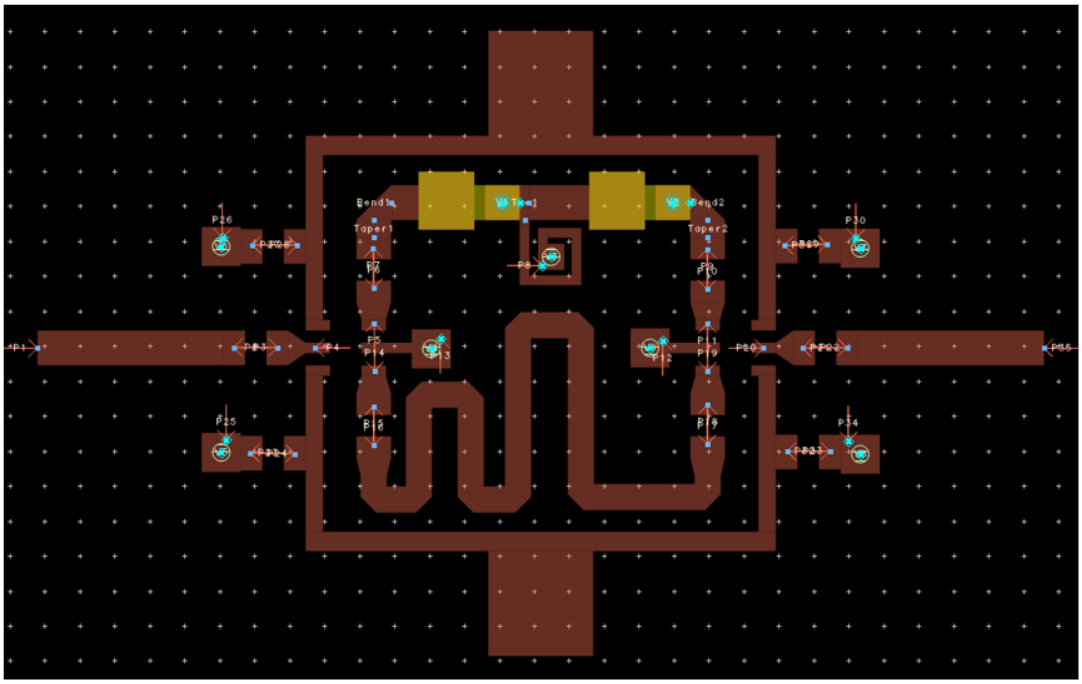

Figure 4.13- Momentum layout of 180° phase shifter with 3D printed lumped components.

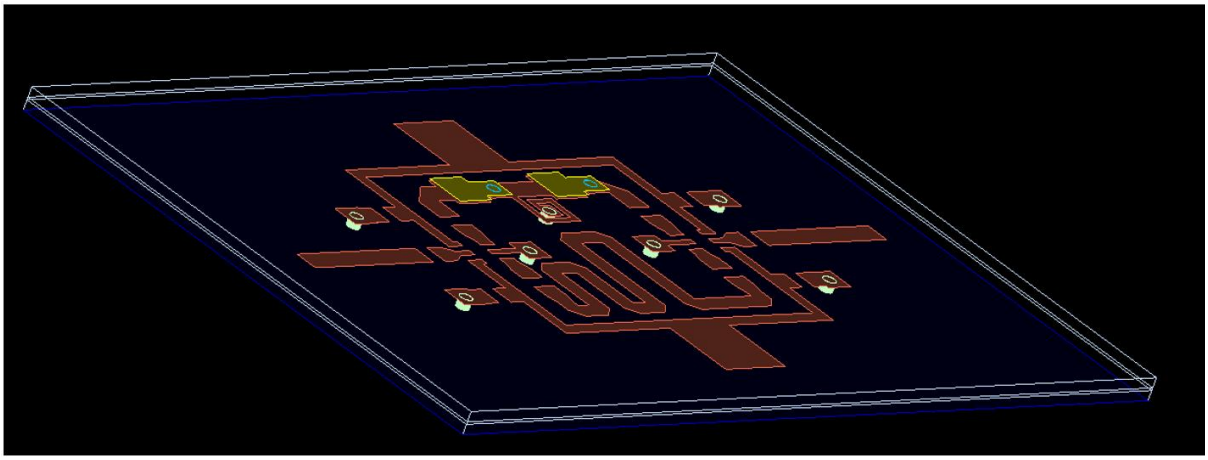

Figure 4.14- 3D view of 180° phase shifter with 3D printed lumped components.

The insertion loss of the thru- and delay- paths, and phase shift is shown in Figure 4.15. As expected the 2.5 dB insertion loss of the thru path is greater than the 1.2 dB insertion loss of the delay path at 2.45 GHz. The discrepancy in insertion loss is partially due to the loss of the 3D

printed capacitors and inductors that make up the high-pass filter path. Figure 4.16 shows the return loss of the phase shifter for both the thru and delay paths.

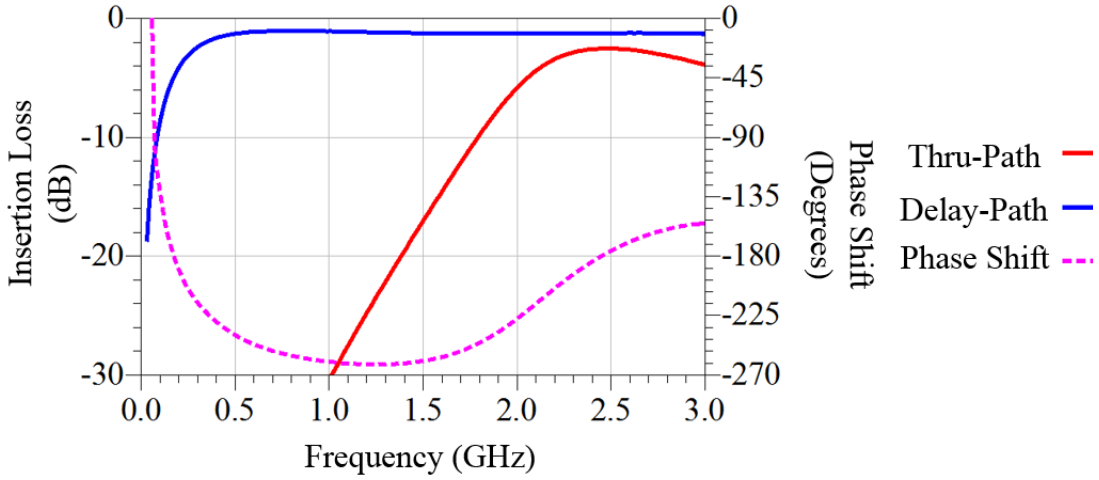

Figure 4.15- IL and phase shift of phase shifter with printed lumped components.

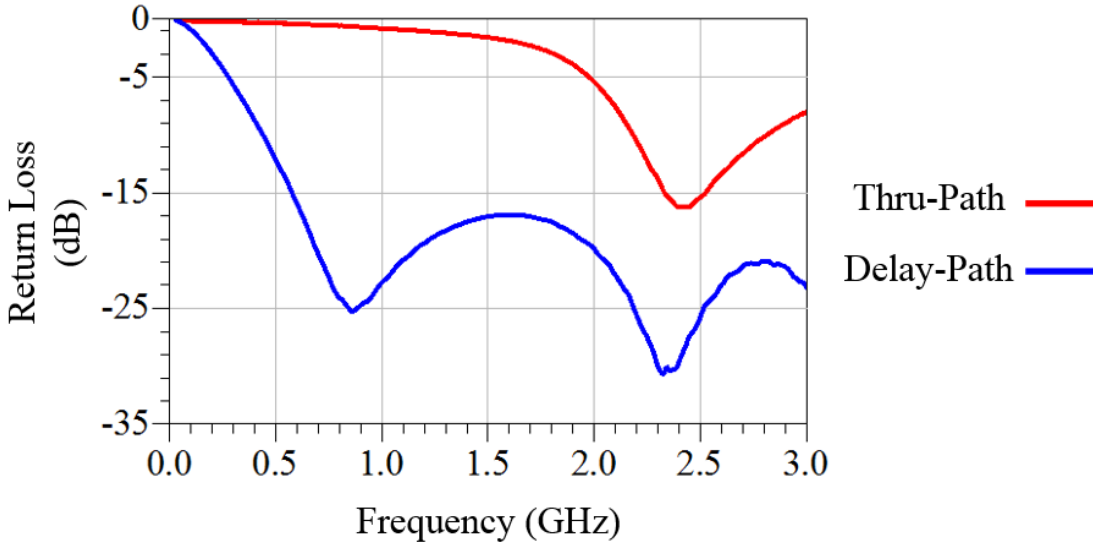

Figure 4.16- Return loss of phase shifter with printed lumped components.

The loss factor of the thru- and delay- paths are shown in Figure 4.17. In addition to heat and radiation losses the data shown below also includes switch loss which accounts for a good portion of the overall loss of the circuit.

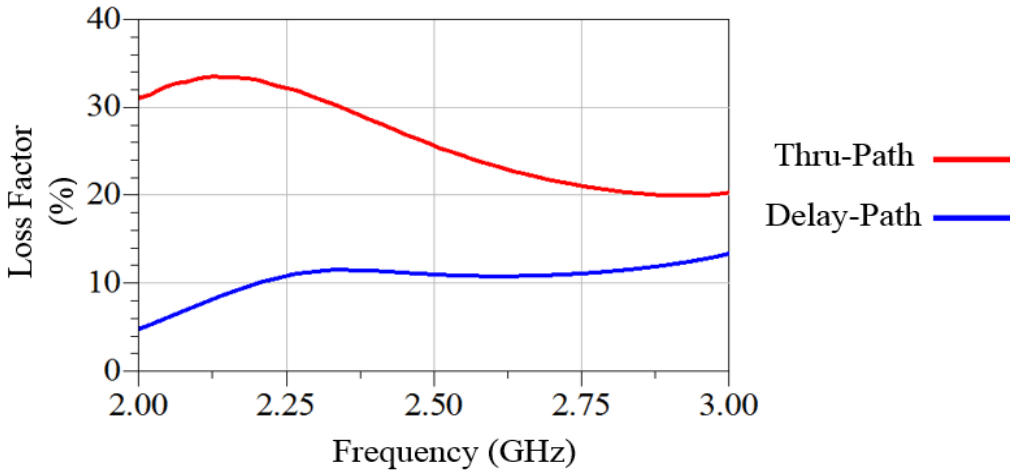

Figure 4.17- Loss factor of phase shifter with printed lumped components.

Table 4.1- Performance comparison of 180° phase shifters. 180° phase shifter with printed lumped components and 180° high-pass low-pass phase shifter with ATC/Coilcraft lumped components

	1-bit 180° phase shifter with 3D printed lumped components		1-bit 180° high-pass low-pass phase shifter with ATC/Coilcraft lumped components	
Path	**Thru-**	**Delay-**	**Thru-**	**Delay-**
Insertion Loss (dB)	**2.5**	**1.2**	**1.56**	**1.56**
Return Loss (dB)	**15.5**	**26**	**18**	**22**
Phase Shift (Degrees)	**179**		**182**	
Size (mm^2)	**200**		**180**	

Table 4.1 compares the performance of the 180° phase shifter with printed lumped components to that of the 180° high-pass low-pass phase shifter with ATC/Coilcraft lumped components shown in Chapter 3.

4.5 Conclusion

This chapter demonstrates that a phase shifter with 3D printed lumped components is realizable. Section 4.2 shows that parallel plate capacitors can be constructed by combining CB028 and ABS layers. Section 4.3 shows that spiral inductors are also easy to fabricate by coiling a CB028 transmission line. Lastly, in Section 4.4 it is shown that a phase shifter can be fashioned by combining 3D printed lumped capacitors and inductors. The primary advantage of designing a monolithic circuit using DDM technology is that by doing so a system can be fabricated in a single step. This would decrease per-unit cost, improve production time, and greatly simplify the assembly process. The main constraining factors are the increased loss of the printed components in comparison to their lumped ceramic counterparts and that although small capacitor and inductor values can be reasonably archived using DMM technology, the construction of high value inductors and capacitors for RF applications may be impractical due to their large sizes.

Chapter 5: Conclusion

5.1 Thesis Summary

The use of direct digital manufacturing technology has proven to be a feasible and cost effective process for the fabrication of digital RF phase shifters. As presented in Section 3.2, the performance of 3D printed phase shifters comes close, but does not currently match that of their PCB counterparts. By conducting a detailed loss analysis of this 3D printed and PCB devices Chapter 3 explains the discrepancies in performance between the two technologies. The low conductivity of CB028 silver ink in comparison to copper, and the inability to print dielectric substrates with low surface roughness are shown to be the main constraining factors to direct digital manufacturing technology.

By analyzing the behavior of 3D printed parallel plate capacitors and spiral inductors, Chapter 4 demonstrates that the fabrication of phase shifters with 3D printed lumped components is a possibility. Parallel plate capacitors can be fabricated by stacking layers of CB028 and ABS. Spiral inductors can also be constructed by coiling a CB028 transmission line on an ABS substrate. The main disadvantages to 3D printed capacitors is that the low dielectric constant of ABS makes the fabrication of large capacitance values impractical due to their large size.

5.2 Recommendations for Future Works

Further areas of study include:

1. Fabricating the 3D printed capacitor, and inductor shown in chapter 4 and compare their performance to the simulations.

2. Fabricate the 3D printed phase shifter design in section 4.4 and compare its performance to the simulations.
3. Investigate ways to integrate materials with higher dielectric constants into a design to miniaturize the capacitor design in chapter 4.

References

[1] 3D Printing Industry [Online]. Available: http://3dprintingindustry.com/2015/02/26/12-things-we-can-3d-print-in-medicine-right-now/.[Accessed: 18-Feb-2015].

[2] Javelin [Online]. Available: http://www.javelin-tech.com/3d-printer/industry/.[Accessed: 18-Feb-2015].

[3] J. Adams, et al. "Conformal Printing of Electrically Small Antennas on Three-Dimensional Surfaces." Advanced Materials 23, no. 11 (n.d.): 1335-1340. Science Citation Index, EBSCOhost (accessed March 25, 2015).

[4] J. O'Brien, E. Rojas, T. Weller, M. Newton and D. Silva, "A Switched-Line Microwave Phase Shifter Fabricated with Additive Manufacturing," 2013 IMAPS Symposium, March 2013

[5] Excell, Jon. "The rise of additive manufacturing". The engineer. [Online]. Available: http://www.theengineer.co.uk/in-depth/the-big-story/the-rise-of-additive-manufacturing/1002560.article.[Accessed: 5-Apr-2015].

[6] Nicholas Arnal et al, "3D Multi-Layer Additive Manufacturing of a 2.45 GHz RF Front End" International microwave symposium (IMS), Phoenix, Arizona, 2015

[7] [Online]. Available: http://www.stratasys.com/3d-printers/technologies/fdm-technology.[Accessed: 5-Apr-2015].

[8] [Online]. Available: http://www.nscrypt.com/direct-print-smartpump/index.php.[Accessed: 5-Apr-2015].

[9] [Online]. Available: http://www.nscrypt.com/micro-dispensing-systems-equipment/direct-print-3dn-machines/index.php.[Accessed: 5-Apr-2015].

[10] [Online]. Available: http://www.odyseus.nildram.co.uk/RFMicrowave_Circuits_Files/Phase_%20Shifter.pdf.[Accessed: 5-Apr-2015].

[11] The microwave engineering handbook, Vol.2, Van Nostrand Reinhold, New York, NY, 1993, pp.29- 40

[12] Iulian Rosu, YO3DAC / VA3IUL. [Online]. Available: http://www.qsl.net/va3iul/.[Accessed: 5-Apr-2015].

[13] [Online]. Available: http://www.microwaves101.com/encyclopedias/phase-shifter-rms-amplitude-error.[Accessed: 7-May-2015].

[14] N. Arnal et al. ‘3D Multi-Layer Additive Manufacturing of a 2.45 GHz RF Front End’, in *International Microwave Symposium (IMS)*, Phoenix, AZ, 2015.

[15] M. F. Cordoba-Erazo, E. A. Rojas-Nastrucci and T. M. Weller, “Simultaneous RF Electrical Conductivity and Topography Mapping of Smooth and Rough Conductive Traces Using Microwave Microscopy to Identify Localized Variations”, Wireless and Microwave Technology Conference (WAMICON), Cocoa Beach, FL, April, 2015.

[16] Bird, John (2010). Electrical and Electronic Principles and Technology. Routledge. pp. 63–76. ISBN 9780080890562.

Appendix A: Copyright Permission

Below is permission for the use of, Figure 3.1, Figure 3.2, Figure 3.5, Figure 3.7, Figure 3.8, and Figure 3.9.

Copyright Clearance Center RightsLink®

Home | Create Account | Help

IEEE Requesting permission to reuse content from an IEEE publication

Title: 3D multi-layer additive manufacturing of a 2.45 GHz RF front end
Conference Proceedings: Microwave Symposium (IMS), 2015 IEEE MTT-S International
Author: Arnal, N.; Ketterl, T.; Vega, Y.; Stratton, J.; Perkowski, C.; Deffenbaugh, P.; Church, K.; Weller, T.
Publisher: IEEE
Date: 17-22 May 2015
Copyright © 2015, IEEE

LOGIN
If you're a copyright.com user, you can login to RightsLink using your copyright.com credentials. Already a RightsLink user or want to learn more?

Thesis / Dissertation Reuse

The IEEE does not require individuals working on a thesis to obtain a formal reuse license, however, you may print out this statement to be used as a permission grant:

Requirements to be followed when using any portion (e.g., figure, graph, table, or textual material) of an IEEE copyrighted paper in a thesis:

1) In the case of textual material (e.g., using short quotes or referring to the work within these papers) users must give full credit to the original source (author, paper, publication) followed by the IEEE copyright line © 2011 IEEE.
2) In the case of illustrations or tabular material, we require that the copyright line © [Year of original publication] IEEE appear prominently with each reprinted figure and/or table.
3) If a substantial portion of the original paper is to be used, and if you are not the senior author, also obtain the senior author's approval.

Requirements to be followed when using an entire IEEE copyrighted paper in a thesis:

1) The following IEEE copyright/ credit notice should be placed prominently in the references: © [year of original publication] IEEE. Reprinted, with permission, from [author names, paper title, IEEE publication title, and month/year of publication]
2) Only the accepted version of an IEEE copyrighted paper can be used when posting the paper or your thesis on-line.
3) In placing the thesis on the author's university website, please display the following message in a prominent place on the website: In reference to IEEE copyrighted material which is used with permission in this thesis, the IEEE does not endorse any of [university/educational entity's name goes here]'s products or services. Internal or personal use of this material is permitted. If interested in reprinting/republishing IEEE copyrighted material for advertising or promotional purposes or for creating new collective works for resale or redistribution, please go to http://www.ieee.org/publications_standards/publications/rights/rights_link.html to learn how to obtain a License from RightsLink.

If applicable, University Microfilms and/or ProQuest Library, or the Archives of Canada may supply single copies of the dissertation.

BACK | CLOSE WINDOW